GROWTH SUPPRESSION MECHANISM OF CONNEXIN 37 IN RESPONSE TO PHOSPHORYLATION STATE OF THE CARBOXY TERMINUS

By

NICOLE LYNNE JACOBSEN

A Thesis Submitted to The Honors College

In Partial Fulfillment of the Bachelors degree
With Honors in

Nutritional Sciences

THE UNIVERSITY OF ARIZONA

MAY 2012

Approved by:

Janis Burt

Janis M. Burt, PhD

Department of Physiology

Approved by:

Kelly Jackson

Kelly Jackson, MS, RD

Department of Nutritional Sciences

STATEMENT BY AUTHOR

This thesis has been submitted in partial fulfillment of requirements for a degree at The University of Arizona and is deposited in the University Library to be made available to borrowers under rules of the Library.

Signed: Nicole Jacobsen

Growth suppression mechanism of connexin 37 in response to phosphorylation state in the carboxy-terminus

Nicole L. Jacobsen, Tasha K. Nelson, Janis M. Burt
Department of Physiology, University of Arizona, Tucson, Arizona 85719, USA

Connexin 37 (Cx37), profoundly suppresses the growth of rat insulinoma (Rin) cells and requires a functional channel. To determine if the CT is necessary for Cx37-mediated growth suppression, a series of deletions and mutations affecting the availability of putative phosphorylation sites in the region of 273-333 of Cx37 were generated. Truncation at P273 alleviated the growth suppressive effect of Cx37 while retaining channel functionality. Interestingly, substate behavior is lost in iRin37-273tr. Based on the observation of run-down behavior in Cx37-wt channels consistent with dialysis of PKC, TPA and BIM treatment of Cx37-wt channels revealed that PKC activation generates a higher incidence of high conductance channels whereas BIM treatment results in the converse. Exploiting this observation, a S-Ax3 mutation targeting known MAPK and PKC sites aligned from Cx43, was generated. However, channels are able to reside in the sub-conductance state and cells are anti-proliferative. Four additional serine to alanine mutations at putative phosphorylation sites (>90%) were made to generate an S7A mutation and did not dispel the growth suppressive effect of Cx37. A phosphomimetic S7D mutation appears to induce cell death. Based on these data, it appears that substate behavior regulated by the CT is indicative growth suppression by Cx37.

Key words: gap junction, connexin 37, cell cycle, phosphorylation

Growth suppression mechanism of connexin 37 in response to phosphorylation state in the carboxy-terminus

Nicole L. Jacobsen, Tasha K. Nelson, Janis M. Burt
Department of Physiology, University of Arizona, Tucson, Arizona 85719, USA

Introduction.

Gap junction channels are composed of one of more of the 21 members of the connexin (Cx) gene family in humans (Martínez et al., 2011) Six connexin monomers assemble into a connexon, or hemichannel. Hemichannels in neighboring cells dock to form a complete gap junction channel, which supports direct communication of ions and small molecules up to 1000 daltons in size between cells. Separated into different subfamilies based on similarities between amino acid sequences, the majority of connexins are categorized in the α- or β-subfamilies (Kyle et al., 2009). All connexin proteins share a comparable secondary structure with four transmembrane, two extracellular and three cytosolic domains (Kardami et al., 2007). While membrane spanning and extracellular domains assist in connexon formation, the intracellular amino-terminus, cytoplasmic loop, and carboxy-terminus (CT) participate in regulation of cellular processes such as development, growth, and differentiation (Söhl and Willecke, 2007; Nakamura et al., 1998) by regulating channel function or interaction of the channel proteins with other proteins necessary for these cellular processes.

Historically, gap junctions were thought to support homeostasis and growth by providing a regulated pathway for intercellular exchange of growth regulatory substances and signaling molecules (Burra and Jiang, 2011). Thus, an inverse relationship between gap junction intercellular communication and cell proliferation was observed for several connexin isoforms, including Cx26, Cx32, and Cx43 (Dang et al., 2006). In the last decade or so, it has become clear that in addition to providing this intercellular communication pathway, connexins coordinate tissue growth and homeostasis by mediating transmembrane diffusion of small molecules through hemichannels and by interacting with growth regulatory proteins via the CT domain (Haefliger et al., 2003; Goodenough and Paul, 2003; Kardami et al., 2007). All three mechanisms require proper formation and localization of the CT.

The CT domain is a major control center of gap junction function, with phosphorylation controlling channel assembly/degradation as well as gating (Shin et al., 2001; Moreno et al., 2002; Solan and Lampe, 2009). The CT of Cx43, the most extensively studied connexin, contain multiple serines and tyrosines that are known targets for phosphorylation by growth-activated kinases including PKC, MAPK, src, CKII, cdc and others (citation). Phosphorylation in the CT has been observed to modulate chemical gating, but is not required for channel formation (Johnson et al., 2012; Maass et al., 2007). In addition, the CT of Cx43 is a site for interaction with scaffolding and cytoskeletal elements and can participate in transcriptional regulation in a phosphorylation-dependent manner.

We previously reported that Cx37, but not Cx43, profoundly suppresses proliferation of Rin cells (Burt et al., 2008) and further, that Cx37-mediated suppression of proliferation requires channel functionality (Good et al., 2011). The aim of the current study was to determine whether the CT domain is also necessary for Cx37-mediated growth suppression, and if so, whether phosphorylation events in the CT might be the basis for CT-necessity. To address this problem, we used Net PhosK (http://www.cbs.dtu.dk/services/NetPhosK/), NetPhos (http://www.cbs.dtu.dk/services/NetPhos/), and KinasePhos (http://kinasephos.mbc.nctu.edu.tw/) to identify in the CT region of Cx37 residues with a high probability (>90%) for phosphorylation. We then aligned Cx37 with Cx43 to determine which of these sites were conserved and which differed between these proteins. This comparison lead us to compare the function of four mutants of Cx37: a truncation mutant that eliminates residues 273-333 (Cx37-273tr); an alanine for serine substitution at residues 275, 302, 328 (Cx37-S-Ax3), sites conserved in Cx43 at residues 282, 328-330, and 368; an alanine for serine substitution for all high probability sites in the 273-333 region of Cx37 (Cx37-S7A: serines 275, 285, 302, 319, 321, 325, 328); and a serine for aspartate substitution for those same high probability sites (Cx37-S7D). We show that Cx37-273tr fails to suppress proliferation of Rin cells, whereas both S-A mutants retain their growth suppressive properties. Expression of Cx37-S7D induce cell death. All four mutants formed functional gap junction channels, but their open state conductance profile differed considerably. Together, the data indicate that the CT of Cx37 is necessary for Cx37-mediated suppression of Rin cell proliferation. Further, it appears that channel function, per se, is not sufficient for growth suppression; rather a channel able to display substate behavior through phosphorylation dependent mechanisms is necessary for Cx37-mediate growth suppression.

Materials and Methods.

Antibodies and reagents. All general chemicals, unless otherwise noted, were purchased from Sigma-Aldrich Chemical. Two Cx37 antibodies [αCx37-18264 (A. Simon et al., 2006) and αCx37-ADI (Alpha-Diagnostics)] were used both for immunoblots and immunofluorescence for all mutants except 273tr. Instead, V5 antibody (Invitrogen) was used in both of these applications for 273tr mutant. Positope (Invitrogen) was used as a positive control for V5 antibody on western blots. Cy3-conjugated anti-rabbit IgG (Jackson Immunoresearch) was used for immunofluorescence. Horseradish peroxidase-conjugated secondary antibodies and enhanced chemiluminescence strategies were utilized in immunoblotting [SuperSignal West Pico or Femto Systems (Pierce), as appropriate].

Cell culture and expression vectors. Communication-deficient rat insulinoma cells [Rin1046-38 (Clark et al., 1990; Gazdar et al., 1980)] obtained from R. Lynch (University of Arizona) were maintained in RPMI 1640 medium supplemented with 10% fetal bovine serum (FBS) or 10% FetalPlex (FP) (Gemini Bioproducts, Sacramento, CA) and antibiotics (300 µg/ml penicillin and 500 µg/ml streptomycin) at 37°C in a humidified, 5% CO_2 incubator. Rin cells were transfected with pTET-ON vector using Lipofectamine according to the manufacturer's instructions (Burt et al., 2008). iRin cells were dilution subcloned and selected in G418 (300 µg/ml). Induction of protein expression was obtained with 2 µg/ml of doxycycline except for S7A and S7D mutants (4 µg/ml doxycycline).

Generation of mutant connexins. wtCx37 and all of the mutants have been ligated into the pTRE2hygro vector (Clontech), part of an inducible system in conjunction with the pTET-ON vector. This system allows for a transcription factor to be made in the presence of doxycycline and this factor turns on the transcription of the gene of interest in the pTRE2 vector.

273tr +V5 deleted amino acids 273-333 with the addition of a V5 tag using an appropriately designed 3- end primer as described in Fig. 1. The primer includes a BamHI restriction site, a V5 tag, and a stop codon. This 273tr+V5 primer was used in a standard PCR reaction (94^{o}- 30sec, 55^{o}-30sec,72^{o}-1 min, 30cycles) with pTRE2F primer

(5’cgcctggagacgccatcc3’) to amplify the DNA fragment. After Qiaquick purification (Qiagen), this was then BamHI/NotI digested and ligated into pTRE2hygro vector (Clontech).

The S-Ax3, S7A, and S7D mutations were generated sequentially to introduce mutations using the QuikChange Site Directed Mutagenesis Kit (Stratagene) using the primers listed in Table 1. The sixth and final mutation reaction to generate both septutple mutants utilized Multisite QuikChange (Stratagene).

All sequences were confirmed at the University of Arizona UAGC Sequencing Facility. Plasmids were transfected into iRin cells using Lipofectamine according to the manufacturer’s instructions. Stably transfected cells were selected in 100 μg/ml hygromyocin before subcloning.

Immunoblotting. Whole cell protein was isolated as previously described (Burt et al., 2008) and its protein content determined using the BCA assay (Pierce Chemical). Samples (5-50 μg protein) were electrophoresed on 12% SDS-PAGE gels and transferred onto nitrocellulose membranes before being blocked with 5% NFDM (non-fat dry milk) and detected by either Cx37 or V5 antibodies using chemiluminescence. Blots were visualized using Kodak Imagestation 2000.

Proliferation. Cells were initially plated at low density (~3,125 cells/cm^2) in triplicate in a 6-well plate. 24 h after plating, doxycycline [2 μg/ml for all cell lines except S7A and S7D (4 μg/ml)] was added to three of the six wells allocated to each time point. Cells were fed every 48 h with or without doxycycline, if appropriate. For a total of 21 days, every 3 days the cells in each well designated for each time point were harvested using trypsin. The number of cells per well was determined using a Cellometer (Nexcelom) after harvesting.

Serum Deprivation and FACS Analysis. Cells were plated at 1×10^6 cells per 100mm plate in standard culture medium. 24 h later, medium was refreshed with serum free medium (control was maintained in serum-containing medium). After 48 hours, all plates were induced with doxycycline at concentrations suitable for maximum induction. Another 24 hours later, cells were harvested for cell cycle analysis as previously described (Burt et al., 2008) or returned to serum-containing medium with doxycycline. Cells released from serum deprivation were harvested and analyzed for cell cycle position 4, 10, 24, 48, 72, and 96 hours after serum restoration using propidium iodide staining. Because Cx37-wt has been reported to reduce adhesivity in some cell types (Wong et al., 2006) and induce apoptosis in others (Seul et al., 2004), the position of unattached cells in the cell cycle was also evaluated in the S7D mutant. FACS analysis was performed at the AZCC/ARL-Division of Biotechnology Cytometry Core Facility.

Electrophysiology. Stably transfected iRin37, iRin37-273tr, iRin37-S-Ax3, iRin37-S7A, and iRin37-S7D cells were plated at low density on coverslips. After 24 hours, cells were treated with doxycycline at a concentration to induce maximal expression. Coverslips were mounted in a custom-made chamber and the cells were immersed in an external solution containing (in mM): 142.5 NaCl, 4 KCl, 1 MgCl2, 5 glucose, 2 Napyruvate, 10 HEPES, 15 CsCl, 10 TEA-Cl, 1 $BaCl_2$, 1 $CaCl_2$. Junctional Conductance was determined as previously described (Burt et al., 2008; Kurjiaka et al., 1998) using dual whole cell voltage-clamp techniques and patch pipets containing an internal solution comprised of (in mM): 124 KCl, 14 CsCl, 9 HEPES, 9 EGTA, 0.5 $CaCl_2$, 5 glucose, 9 TEA-Cl, 3 $MgCl_2$, 5 Na_2ATP. Electrodes used were from 3-10 MΩ. Single channel conductance was recorded using halothane if recordings above 1nS. In PKC activity studies, TPA (PKC activator was applied for 30 minutes at room temperature at a concentration of 50ng/ml before recordings were taken. BIM (PKC inhibitor) was applied for 60 minutes at room temperature before recording at a concentration of 0.2 μM. Transition measurement events lasted 50 µs, and filtered at 50Hz to reduce noise. Data was analyzed in 10pS bins to calculate relative frequency before being corrected for baseline. Cell pairs were not in the external solution for more than 60 minutes at a time. For the all points histograms, all points from a 2 second single channel record are compiled into 10pS data points to generate histogram. Peaks are identified and then calculated based on a 25mV driving force.

Statistics. Statistical comparisons of all data were performed using unpaired, two-tailed Student's t-tests. Significant differences were taken as $P<0.05$. Error bars represent mean ± s.e.m.

Results.

Mutant forms of Cx37 assemble into gap junctions. To determine the importance of different residues within the CT that may be involved in regulating the growth suppression witnessed by some connexins, we studied Cx37 and different mutations in the CT altering the sequence of the protein. We needed a series of mutations that would selectively modify the accessibility of phosphorylation sites while preserving the integrity of channel formation and structure. We deleted a portion of the cytoplasmic tail in Cx37 after amino acid 273 so as to not disrupt the connexin's structural components but eliminated many serines available for kinase activity. Also, generating S-Ax3, S7A, and S7D substitution mutants, we were able to evaluate which specific amino acids in the deleted region that might serve as sites for kinase activity, thereby regulating the function of the protein. Gap junction formation and function was studied in Rin cells stably transfected with Cx37 or one of the deletion and substitution mutant forms of Cx37. After selection of high and low expressing clones of mutant cell lines, maximum induced protein expression with doxycycline was evaluated in a dose-dependent fashion. With a 2 ug/ml concentrations at 24 hours after addition of doxycycline exhibiting maximal protein expressing in 273tr and S-Ax3 cell lines, protein expression was comparable to the previously characterized iRin37F (Fig. 2A). 4 ug/ml doxycycline was sufficient for maximal and similar expression to wt in S7A and S7D cell lines (Fig. 2B). All mutant cell lines expressed protein levels between the high expressing iRin37F and low expressing iRin37-2 clones (Fig. 2).

Macroscopic junctional conductance recordings indicated that all cell lines, whether expressing wt or mutant Cx37, were equally well coupled (Fig. 3A) and formed functional gap junction channels. The mean junctional conductance of iRin37 cell pairs was 3.18±0.71 nS (n=26) 273tr cell pairs was 2.6±0.81nS (n=11). Junctional conductance of S-Ax3 and S7A cell pairs was 6.09±2.76nS (n=8) and 5.12±1.98 nS (n=21) respectively. S7D formed junctions with a significantly higher conductance than wt or the 273tr, S-Ax3, and S7A mutants at 8.88±1.48 nS (n=28). After treatment with PKC inhibitor, BIM, or PKC agonist, TPA, Cx37wt-mediated cell coupling was not affected [BIM: 3.95±1.64 nS (n=6); TPA: 2.99±1.36 nS (n=7)] (Fig. 3B). Although electrical coupling provides information concerning formation of gap junction channels, it does not indicate if the channel is in a fully open or partially closed conformation or if the open states of the channel have changed due to alterations in the wild-type protein.

Dephosphorylated Cx37 predominately resides in higher conductance state. Next, we evaluated the effect mutation of putative phosphorylation sites on single channel behavior. 273tr appears to be able to open fully and remains in this state more stably than wt (Fig. 4B). Versus the truncation mutant, S7A channels rarely open to the documented fully open configuration for Cx37wt (360pS). However, S7A frequently opens to 240pS configuration and has an increased dwell time in this state. iRin37-wt and S7D seem to reside in a substate configuration routinely.

Using single channel event amplitude histograms, the impact of these mutations on conductance of stable open states could be evaluated. 273tr shows a greater tendency than Cx37-wt to reside in the fully open state. The S7A mutant resides more stably at open state corresponding to 80pS (like wt) and 240pS (Fig. 5C). The S7D mutant mimics Cx37wt, with a substate of about 90pS, similar to Cx37wt (Fig. 5D). In the S-Ax3 mutant, frequencies of fully open and subconductive states were observed similarly suggesting a behavior dissimilar to either the more "phosphorylated" (iRin37F, S7D) or less "phosphorylated: (273tr, S7A) forms (Fig. 5B).

iRin37-F cell line was treated with a PKC inhibitor and agonist in order to evaluate if activation or suppression of PKC-mediated phosphorylation affected the conductance state of the channel. When treated with BIM, channels predominately resided in the smaller conductance states while converse treatment with TPA triggered a shift to a more open conformation (Fig. 6). BIM treatment was hypothesized to mimic the behavior of the S-Ax3 mutation. However, S-Ax3 cells experienced comparable levels of open and substate conformation suggesting additional phosphorylation sites responsible for maintenance of smaller conductance states as seen in the wt protein.

Variability of proliferation among mutants. To determine the role of the CT and putative phosphorylation sites therein in mediating the growth suppressive properties of Cx37, we compared the proliferation of each mutant, both induced and uninduced, to iRin37 over a 21 day time course. As shown in Fig. 7A, 273tr cells grew in an exponential pattern, similar to the uninduced iRin37. Periods of exponential growth (linear regions on a logarithmic plot) were determined for each of these cell types. Cell cycle time was calculated for periods of exponential growth as (t2-t1)*(log(2)/log(q2/q1)) (where t is time and q is number of cells) using a 3- or 6-day window of analysis as previously described (Burt et al., 2008). Cx37-wt expressing cells doubled every 8 or 9 days before a transition at day 12 to a shorter doubling time of 2-3 days. The growth permissive 273tr cell line exhibited a shortened cell cycle time of 1.5 or 2 days throughout the 21-day period. In contrast, The S-Ax3 mutant was growth suppressed but escaped the growth suppression late in the growth curve (n=3) (Fig. 7B). Also, both the S7A mutant and the phospho-mimetic mutant, S7D, were significantly growth suppressed throughout the entire 21-day period (n=4) (Fig. 7C-D)

Cell cycle analysis of S7A and S7D revealed growth arrest and possible apoptosis. Next, we sought to determine the cell cycle position of S7A and S7D cells using Fluorescence Activated Cell Sorting. After cells were serum deprived for 72 hours with addition of doxycycline for the last 24 hours, cells were harvested at sequential time points after serum restoration to assess cell cycle position. In iRin37-wt cells, progression from G_1 to S phase was significantly delayed compared to uninduced cells not expressing Cx37 (Burt et al., 2008). In contrast, the S7A and S7D cells experienced minimal progression through the cell cycle throughout the duration of the experiment as evidenced by little change in the distribution of cells in each phase. Interestingly, 24 hours after serum restoration as cells enter the S-phase, the S7D cultures began to accrue a large amount of debris (Fig. 8B), consistent with cell death.

Delayed induction of Cx37-S7D induces cell death. After the elucidation of debris accumulation 24 hours post induction of Cx37-S7D, we compared the growth of S7D cells that were permitted to grow uninduced for 12 days before initiation of Cx37-S7D expression. On day 15, the average number of cells decreased from 1.30×10^6 cells (n=3) on day 12 to 8.85×10^5 cells (n=3) on day 15 (Fig. 9). By day 18, only 5.52×10^4 cells (n=3) remained. When a similar assay was completed in S7A cells, proliferation was slowed but cell number did not decrease (*preliminary data*) as seen in iRin37-S7D.

Discussion.

The growth suppressive properties of connexins have long been studied and recognized as tumor suppressors (Kardami et al., 2007; King and Bertram, 2005; Omori et al., 2001). Previously seen in cell lines expressing Cx26, Cx32, and most extensively in Cx43, sometimes channel function is necessary, other times presence of the CT is sufficient. Growth related kinases modulate and regulate growth and connexin contribution (Solan and Lampe, 2009). However, there still exist a lot of unknowns concerning the growth suppression mechanism of Cx37 (Dang et al., 2003). We recently reported that when expressed in Rin cells, Cx37, but not Cx43, exerted anti-proliferative effects by prolonging all phases of the cell cycle (Burt et al., 2008). The growth arrest was heightened when serum deprived as it became more difficult for cells to pass through the G_1/S checkpoint. Also, we reported that a functional channel is a necessary component to growth regulation in Rin cells (Good et al., 2011). After the introduction of Cx37-T154A, which permitted channel formation but hindered proper channel function, these cells exhibited no growth suppressive effects, suggesting that channel functionality is involved in the Cx37 related mediation of growth. Here, we show the necessity of the CT and the impact of putative phosphorylation sites on channel function and the growth suppressive behavior of Cx37.

The carboxy-terminus has been recognized to influence the number, size, and localization of gap junction plaques thus affecting the function of the connexin (Maass et al., 2007). It can be suggested that if junctions were aberrantly assembled in relation to size and location, growth signaling cascades would be affected as a result. Within the CT of connexins, there are several putative phosphorylation sites in which kinases activate growth factors to promote or inhibit progression through the cell cycle via protein-protein interactions or regulatory protein domains (Solan and Lampe, 2009). As seen in Cx43, inhibition of phosphorylation at S262 (a known PKC site) via a serine to alanine mutation in the carboxy-terminus amplified the restriction of DNA synthesis and resulting proliferation (Doble et al., 2004). Conversely, a phosphomimetic mutation achieved by a serine to aspartic acid substitution reversed the inhibitory effect of Cx43 exhibiting the impact in which availability of kinase activity can alter channel function. After primary sequence alignment of Cx43 with Cx37, many sites were revealed with a high predicted probability of phosphorylation. For instance, PKC-mediated decrease in GJIC targeted at S368 is seen in Cx43 in a number of different cell types, which is consistent with tumorigenesis (Lampe et al., 2000; Solan et al., 2003; Bao et al., 2004; Lampe et al., 2006). Not only is S368 phosphorylation dependent upon PKC activity at that site, but S365 in Cx43 has been shown to regulate the phosphorylation by PKC at S368 (Solan et al., 2007). Additional kinases that have a high predicted probability of phosphorylation in Cx43 are ERK1/2 and CKII. S282 is a predicted ERK1/2 site in Cx43 (Warn-Cramer et al., 1998) and when phosphorylated at this site, there is a decrease in GJIC. Another site of phosphorylation in Cx43 resides at S328, a CKI site. In the combined evaluation of a mutation of serine to alanine at the sites 325, 328, 330 in Cx43 revealed that gap junctions were not assembled properly and their function was severely diminished (Lampe et al., 2006; Remo et al., 2011). After sequence alignment of Cx43 to Cx37, it is predicted that S282 of Cx43 aligns with S275 of Cx37. More over, S365, the regulatory residue of one of the PKC target sites of Cx43 aligns with the predicted S325 in Cx37. Other alignment sites between Cx43 and Cx37 respectively are: S368 in Cx43 with S328 in Cx37 and

S328 in Cx43 with T301 in Cx37. Based on analysis using NetPhos, NetPhosK, and KinasePhos websites, these four sites in Cx37 have a greater than 90% probability of also serving as sites for phosphorylation events also predicted to impact gap junction assembly, function, and localization. Interestingly enough however, not all alignment sites that have been shown to have phosphorylation activity in Cx43 has a high predicted probability of phosphorylation in Cx37. For example, Cx43-S306A has been shown to reduce electrical coupling when expressed in HeLa cells (Procida et al., 2009) but combined use of NetPhos, NetPhosK, and KinasePhos have predicted less than a 1% likelihood of phosphorylation at Cx37-T301. The phosphorylation prediction websites also identified unique sites in Cx37 that do not align with known phosphorylation events in Cx43 that regulate signaling cascades affecting gap junctions. These sites are S254, 285, 302, 319, and 321 and all have a >90% probability of being phosphorylated. While providing a strong link between connexin phosphorylation and cell cycle progression in studies in Cx43, few studies have been conducted altering phosphorylation status in the carboxy-terminus of Cx37 to elucidate its key amino acid residues for growth regulation.

To begin our investigation into growth regulatory sites in Cx37, the truncation mutant eliminates all high probability sites in the CT of Cx37 except S254. After characterization of iRin37-273tr, it revealed that the CT is necessary for Cx37 to exhibit growth suppression. We previously showed that channel functionality is also necessary (Good et al., 2011) to retain growth suppression in Rin cells. While 273tr forms functional channels as seen by macroscopic conductance levels, these channels primarily reside in the fully open state instead of a CT-dependent substate. Run-down behavior, which is a defining aspect of CT-regulated channel function as seen in iRin37-wt, is not seen in iRin37-273tr.

These data imply that regulated channel function is necessary for growth suppression by Cx37. Evidence of such is exhibited through macroscopic conductance experiments and treatment of Cx37-wt channels with BIM or TPA. Run-down behavior was not seen in 273tr channels, which for other channels has been linked to dialysis of key regulatory kinases or phosphatases such as PKC. Due to the elimination of the putative phosphorylation sites, iRin37-273tr no longer exhibits a similar behavior. Not only is run-down behavior lost in the truncation mutant, but when wt channels are treated with TPA or BIM, there is no difference in macroscopic conductance levels between treatment groups or compared to wt. Despite the lack of altered junctional conductance, TPA or BIM treatment altered channel behavior. When treated with PKC inhibitor, cells produced a channel profile comparable to WT whereas treatment with a PKC agonist increased the prevalence of fully open channels. The implications of such remains that in Rin cells, Cx37 has a high probability of being phosphorylated by PKC (and/or kinases that are regulated by PKC) and residing in its fully open state. As a result, undergoing dialysis removes PKC and the channel's open state behavior shifts to a substate.

Given the necessity of regulated channel function for Cx37-mediated growth suppression, the effects of PKC agonists and antagonists on channel function and the alignment of known phosphorylation sites in Cx43 with Cx37, we targeted S275, 302, 325 with serine to alanine mutations. During alignment of Cx43 to Cx37, the amino acid residues of Cx43 S325, 328, 330 align with T301, S302, and S303 of Cx37 respectively. However, as stated earlier, T301 has a low probability of phosphorylation whereas S302 has a greater than 90% likelihood of kinase activity, which is why we chose S302 over T301 for the MAPK/PKC targeted mutant of Cx37. The S-Ax3 mutant fails to relieve growth suppression while also lacking a high incidence of fully open channels. Nevertheless, S-Ax3 channels still occupy a substate behavior distinct from the wt protein. These data suggest that Cx37 is growth suppressive when not phosphorylated at these sites and that a hallmark of the growth suppressive channel is any substate behavior.

The S7A mutant substitutes alanine for all serines in the 273-333 deletion region of the truncation with a predicted probability for phosphorylation >90% by NetPhos, NetPhosK, and KinasePhos websites. This mutant is also growth suppression contradictory to our hypothesis. Like the wt and S-Ax3 mutants, S7A channels reside primarily in sub-conductance states, with very few transitions to the fully open state. Interestingly, the proliferation curves for S7A, unlike S-Ax3 show no escape from growth suppression late in the growth curve.

The implications of S-Ax3 and S7A mutants is that phosphorylation at one or more sites in the CT is necessary for channels to occupy the fully open state for periods long enough to be measured as a stable, fully open channel. In addition, in combination with the 273tr data, the fully open channel is not sufficient for growth suppression but instead substate behavior is indicative of growth suppression. Further, S7A data suggest additional regulatory sites with in the 273-333 region of the CT. Alternatively, unique combinations of these identified serine sites, or additional sites outside this domain could be involved in both growth suppression and substate behavior.

Based on the S7A data, we hypothesized that S7D would behave opposite to S7A. However, the growth curves appeared to counter this expectation. The delayed induction proliferation assays and FACS data, in addition to visual inspection of the cells, all suggest this mutant induces cell death. Interestingly, before cell death is evident around 48 hours post induction, this mutant forms gap junction channels whose conductance profile is indistinguishable from the wt. With a channel profile similar to wt yet cells undergo cell death, S7D cells could be acting through several possibilities: (1) Cx37 hemichannels may be the growth regulatory form of this protein. This means, if the open probability or number of open channels use signaling more often in S7D than wt or S7A, this transmembrane signaling may be detrimental. This mechanism seems possible since expression level and coupling is higher despite the existence of small channels. (2) The mutated channel protein could fail to interact with anti-apoptotic signaling cascade elements, or alternatively sequester these elements such that they cannot prevent cell death. While there are numerous other possibilities, these seem the most likely.

Altogether, our data reflect that the CT is necessary for growth suppression of Rin cells by Cx37 with maintenance of channel function. While presence of the CT is not sufficient, channels must be functioning and must be regulated as seen by substate behavior. It is still unclear whether selectivity might differ for different open state, or for the same open state but differing phosphorylation state. It is also unclear which additional sites might be involved, if any, or if combinations of these existing sites work together to mediate growth suppression. Finally, it is unclear if there are interacting proteins critical to growth suppression and cell survival that differe across these mutations.

Acknowledgements.

I would like to thank Dr. Burt for all of her input and guidance throughout this project. Also, I would like to thank Tasha Nelson for continual help with experimental design and trouble-shooting. Additionally, a special thanks to the other remaining members of the Burt Lab for their assistance and friendship.

References.

Bao X, Altenberg GA, and Reuss L. Mechanism of regulation of the gap junction protein connexin 43 by protein kinase C-mediated phosphorylation. *Am J Physiol Cell Physiol* 286: C647-C654, 2004.

Burra S and Jiang JX. Regulation of cellular function by connexin hemichannels. *Int J Biochem Mol Biol* 2 (2): 119-128, 2011.

Burt, JM, TK Nelson, AM Simon, and JS Fang. Connexin 37 profoundly slows cell cycle progression in rat insulinoma cells. *Am J Physiol Cell Physiol* 295: C1103-C1112, 2008.
Clark SA, Burnham BL, Chick WL. Modulation of glucose-induced insulin secretion from rat clonal beta-cell line. *Endocrinology* 127: 2779-2788, 1990.

Dang X, Doble BW, and Kardami E. The carboxy tail of connexin-43 localizes to the nucleus and inhibits growth. *Molecular and Cellular Biochemistry* 242: 35-38, 2003.

Dang X, Jeyaraman M, and Kardami E. Regulation of connexin-43-mediated growth inhibition by a phosphorylatable amino-acid is independent of gap junction-forming ability. *Mol and Cell Biochem* 289: 201-207, 2006.

Doble BW, Dang X, Ping P, Fandrich RR, Nickel BE, Jin Y, Cattini PA, and Kardami E. Phosphorylation of serine 262 in the gap junction protein connexin-43 regulates DNA synthesis in cell contact forming cardiomyocytes. *Jour Cell Sci* 117: 507-514, 2004.

Gazdar AF, Chick WL, Oie HK, Sims HL, King DL, Weir GC, Lauris V. Continuous, clonal, insulin- and somatostatin-secreting cell ines established from a transplatable rate islet cell tumor. *Proc Natl Acad Sci USA* 77: 3519-3523, 1980.

Good ME, Nelson TK, Simon AM, and Burt JM. A functional channel is necessary for growth suppression by Cx37. *Jour of Cell Sci* 124: 2448-2456, 2011.

Goodenough DA, and Paul DL. Beyond the gap: functions of unpaired connexon channels. *Nat Rev Mol Cell Biol* 4: 285-294, 2003.

Haefliger JA, Nicod P, and Meda P. Contribution of connexins to the vascular wall. *Cardio Res* 62: 345-356, 2004.

Johnson RG, Reynhout JK, TenBroek EM, Quade BJ, Yasumura T, Davidson KG, Sheridan JD, Rash JE. Gap junction assembly: roles for the formation plaque and regulationby the C-terminus of connexin43. *Mol Biol Cell* 23 (1): 71-86, 2012.

Kardami E, Dang X, Iacobas DA, Nickel BE, Jeyaraman M, Srisakuldee W, Makazan J, Tanguy S, Spray DC. The role of connexins in controlling cell growth and gene expression. *Prog Biophys Mol Biol* 94: 245-264, 2007.

King TJ and Bertram JS. Connexins as targets for cancer chemoprevention and chemotherapy. *Biochem Biophys Acta* 1719: 146-160, 2005.

Kurjiaka DT, Steele TD, Olsen MV, Burt JM. Gap junction permeability is diminished in proliferating vascular smooth muscle cells. *Am J Physiol Cell Physiol* 275: C1674-C1682, 1998.

Kyle JW, Berthoud VM, Kurutz J, Minogue PJ, Greenspan M, Hanck DA, Beyer EC. The n terminus of connexin 37 contains an α-helix that is required for channel function. *J Biol Chem* 284: 20418-20427, 2009.

Lampe PD, Cooper CD, King TJ, Burt JM. Analysis of phosphorylation of connexin43 at S325/328/330 in normoxic and ischemic heart. *J Cell Sci* 119: 3435-3442, 2006.

Lampe PD and Lau AF. The effects of connexin phosphorylation on gap junctional communication. *Int J Biochem Cell Biol* 36: 1171-1186, 2004.

Lampe PD, TenBrock EM, Burt JM, Kurata WE, Johnson RG, Lau AF. Phosphorylation of connexin43 on serine368 by protein kinase C regulates gap junctional communication. *Jour Cell Biol* 149(7): 1503-1512, 2000.

Maass K, Shibayama J, Chase SE, Willecke K, Delmar M. C-terminal truncation of connexin-43 changes number, size, and localization of cardiac gap junction plaques. *Circ Res* 101: 1283-1291, 2007.

Martinez AD, Maripillan J, Acuna R, Monigue PJ, Berthoud VM, Beyer EC. Different domains are critical for oligomerization compatibility of different connexins. *Biochem J* 436: 35-43, 2011.

Moreno AP, Chanson M, Anumonwo J, Scerri I, Gu H, Taffet SM, and Delmar M. Role of the carboxyl terminal of connexin43 in transjunctional fast voltage gating. *Circ Res* 90: 450-457, 2002.

Nakamura Ky, Inai T, Nakamura Ke, and Shibata Y. Distribution of gap junction protein connexin 37 in smooth muscle cells of the rat trachea and pulmonary artery. *Arch Histol Cytol* 62: 27-37, 1999.

Omori Y, Dagli MLZ, Yamakage K, and Yamasaki H. Involvement of gap junctions in tumor suppression: analysis of genetically-manipulated mice. *Mut Res* 477: 191-196, 2001.

Remo BF, Qu J, Volpicelli FM, Giovannone S, Shin D, Lader J, Liu FY, Zhang J, Lent DS, Morley GE, Fishman GI. Phosphatase-resistant gap junctions inhibit pathological remodeling and prevent arrhythmias. *Circ Res* 108 (12): 1459-1466, 2011.

Seul KH, Kang KY, Lee KS, Kim SH, and Beyer EC. Adenoviral delivery of human connexin37 induces endothelial cell death through apoptosis. *Biochem and Biophys Res Comm* 319: 1144-1151, 2004.

Shin JL, Solan JL, and Lampe PD. The regulatory role of the c-terminal doman of connexin43. *Cell Comm & Adhes* 8(4-6): 271-275, 2001.

Simon AM, Chen H, Jackson CL. Cx37 and Cx43 localize to zona pellucida in mouse ovarian follicles. *Cell Commun Adhes* 13: 61-77, 2006.

Sohl G and Willecke K. Gap junctions and the connexin protein family. *Cardio Res* 62: 228-232, 2004.

Solan JL, Fry MD, TenBroek EM, Lampe PD. Connexin43 phosphorylation at S368 is acute during S and G2/M and in response to protein kinase C activation. *J Cell Sci* 116: 2203-2211, 2003.

Solan JL and Lampe PD. Connexin43 phosphorylation: structural changes and biological effects. *Biochem J* 419: 261-272, 2009.

Solan JL and Lampe PD. Key connexin 43 phosphorylation events regulate the gap junction life cycle. *J Membr Biol* 217(1-3): 35-41, 2007.

Warn-Cramer BJ, Cottrell GT, Burt JM, Lau AF. Regulation of connexin-43 gap junctional intercellular communication by mitogen-activated protein kinase. *J Biol Chem* 273 (15): 9188-9196, 1998.

Wong CW, Christen T, Roth I, Chadjichristos CE, Derouette JP, Foglia BF, Chanson M, Goodenough DA, and Kwak BR. Connexin37 protects against atherosclerosis by regulating monocyte adhesion. *Nat Med* 12: 950-954, 2006.

Figures.

Figure 1. Visual representation of Cx37 sequence with mutation sites of cytoplasmic tail highlighted and list of primers used to generate mutants. A) P273 (blue) indicates the beginning of the truncation. S-Ax3 (red squares) denote potential MAPK and PKC activity sites. S7A and S7D (red) have a greater than 90% probability rate of being phosphorylated by relevant kinases. B) List of primers used to generate mutant forms of Cx37 altering phosphorylation site availability.

A)

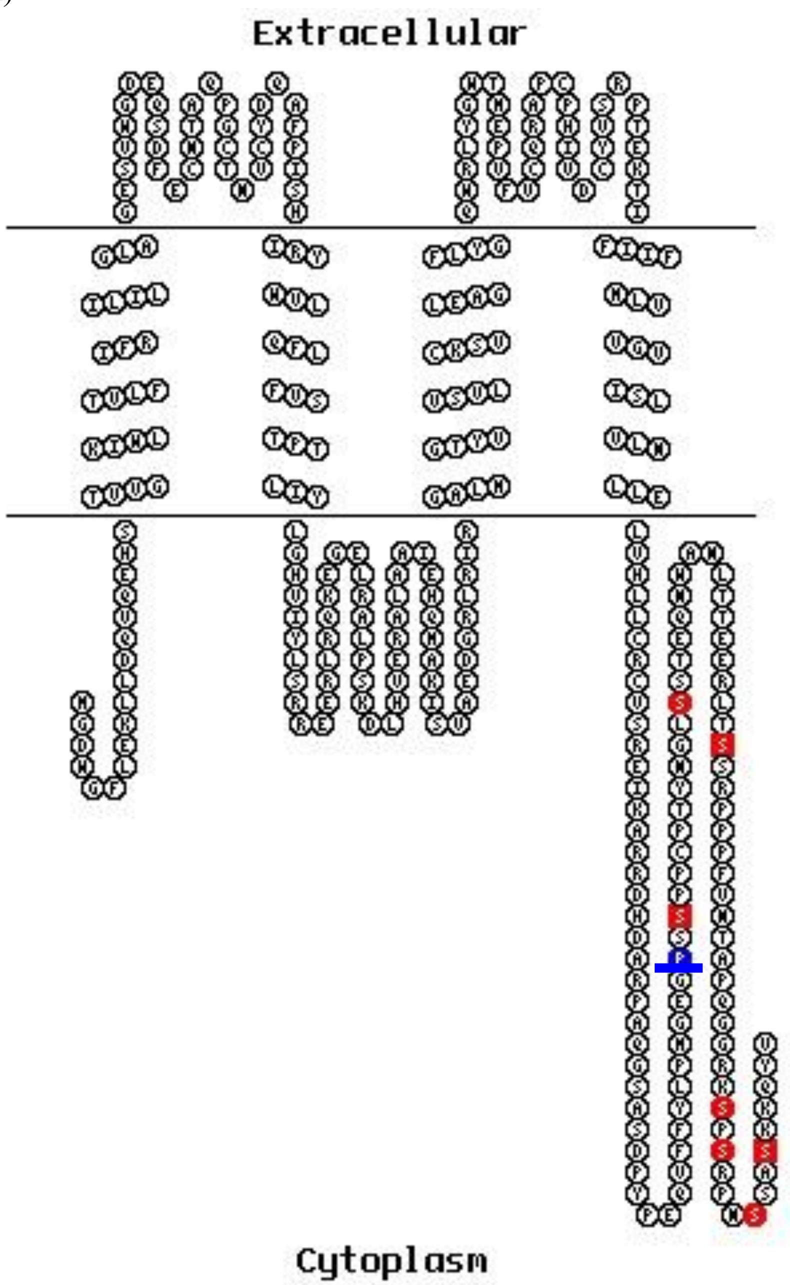

B)

Mutation	Primer sequence	Construct
273tr	5’ctagctagcctacgtagaatcgagaccgaggagaggg ttagggataggcttaccgggtccctcgcccat3’	Cx37-273tr
S302A	F-5’gagagactgaccgcttccagactccc3’ R-5’gggaggtctggaagcggtcagtctctc3’	
S302, 328A	F-5’ccaacagctctgcagccaagaagcagtatgtgt3’ R-5’acacatactgcttcttggctgcagagctgttgg3’	
S275, 302, 328A	F-5’gggaccctctgccccaccgtgtc3’ R-5’gacacggtggggcagagggtccc3’	Cx37-S-Ax3
S275, 285, 302, 328A	F-5’cctacaacgggctcgcttccactgagcagaac3’ R-5’gttctgctcagtggaagcgagcccgttgtagg3’	
S275, 285, 302, 319, 328A	5’cagggtggccgaaaggcacctagccgccccaac3’ R-5’gttggggcggctaggtgcctttcggccaccctg3’	
S275, 285, 302, 319, 321, 325, 328A	F-5’ggcacctgcccgccccaacgcctctg3’ R-5’cagaggcgttggggcgggcaggtgcc3’	Cx37-S7A
S275D	F-5’catgggcgagggaccctctgatccaccgtgtcccacctac3’ R-5’gtaggtgggacacggtggatcagagggtccctcgcccatg3’	
S275, 319D	F-5’cagggtggccgaaaggatcctagccgccccaac3’ R-5’gttggggcggctaggatcctttcggccaccctg3’.	
S275, 319, 328D	F-5’cccaacagctctgcagacaagaagcagtatg3’ R-5’catactgcttcttgtctgcagagctgttggg3’	
S275, 285, 319, 328D	F-5’cctacaacgggctcgactccactgagcagaac3’ R-5’gttctgctcagtggagtcgagcccgttgtagg3’	
S275, 285, 302, 319, 328D	F-5’cacagaggagagactgaccgactccagacctcccccatttg3’ R-5’caaatgggggaggtctggagtcggtcagtctctcctctgtg3’	
S275, 285, 302, 319, 321, 325, 328D	F-5’gccgaaaggatcctgaccgccccaacgactctgcagacaa3’ R-5’cttgtctgcagagtcgttggggcggtcaggatcctttcggc3’	Cx37-S7D

Figure 2. Relative Expression of Cx37 mutants stably transfected in Rin cells. A) For quantification of iRin37-273tr, a standard curve was generated from V5 positope loaded in increasing amounts (lane 1: MW marker; lanes 2-5: 0.25, 0.5, 1, 2 pmols positope; lane 6: iRin37-273tr whole cell lysate 30 ug total protein) B) A standard curve was generated using a similar protocol but instead using Cx37 GST protein as the loading standard for 50 ug each of iRin37-S7A and iRin37-S7D whole cell lysates. C) Results of such experiments of mutant forms of Cx37 has a relative protein expression level between the high expressing wt clone (iRin37-F) and the low expressing wt clone (iRin37-2).

A)

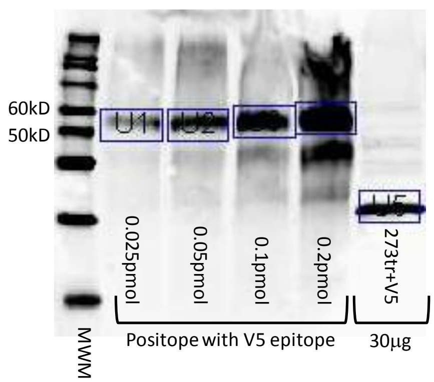

B)

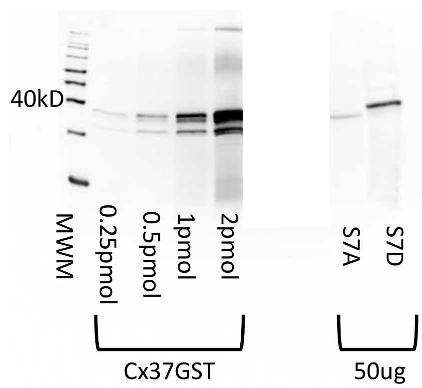

C)

Sample	**pmol/µg**	**Sample size**
iRin37-F	8.21×10^{-3}	Published previously
iRin37-2	4.23×10^{-4}	Published previously
iRin37-273tr	1.37×10^{-3}	1
iRin37-S7A	6.56×10^{-3}	1
iRin37-S7D	1.24×10^{-2}	1

Figure 3. Macroscopic junctional conductance indicating incidence of coupled cell pairs. A) All expressed mutants are as well coupled compared to the wt. B) Treatment with PKC inhibitor or agonist do not affect the coupling of cell pairs in iRin37. *p<.05

A)

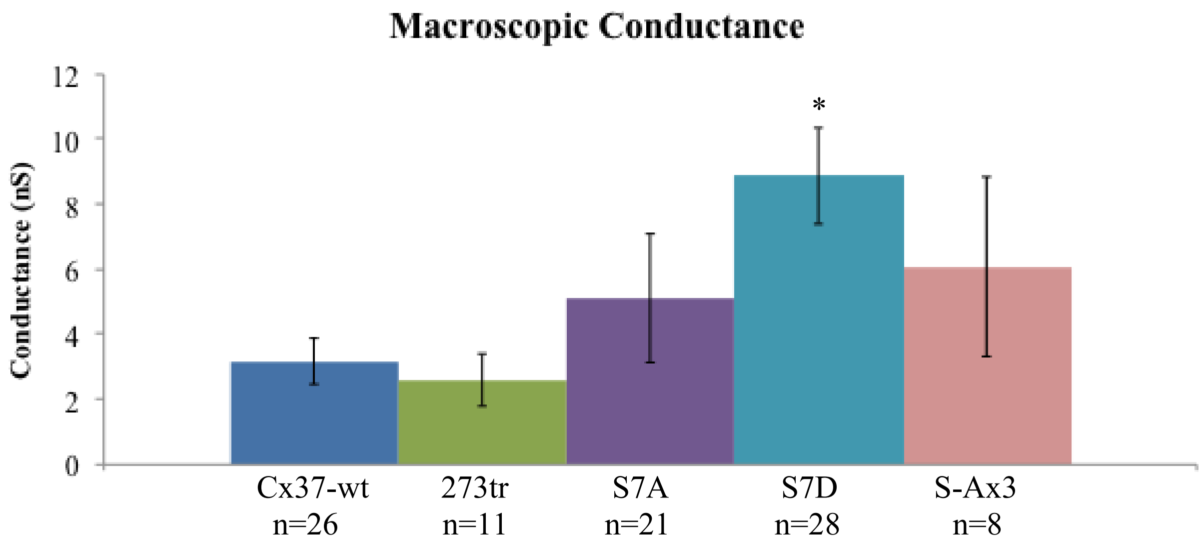

B)

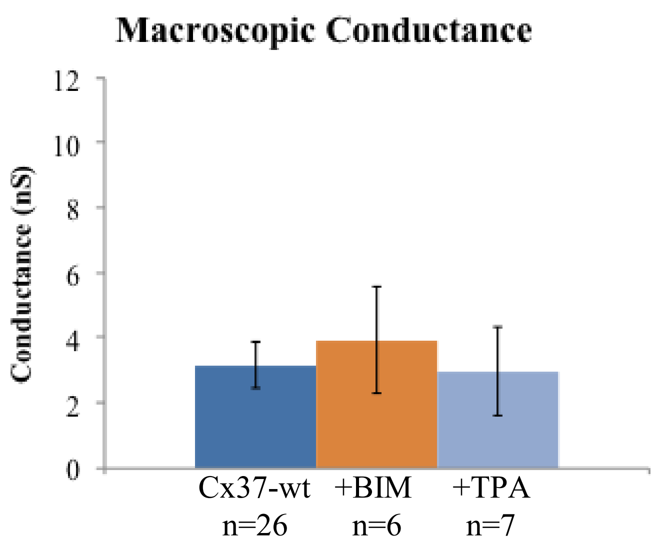

Figure 4. Single channel traces of iRin37-wt and mutant forms of Cx37 with all points histograms indicating 273tr channels have lost substate behavior, which Cx37-wt, S7A, and S7D still possess. Single channel records (2 seconds long) have been baseline adjusted and filtered at 50Hz. Histograms were generated once the peaks were identified based on a 25mV driving force. A) iRin37-wt B) iRin37-273tr C) iRin37-S-Ax3 D) iRin37-S7A E) iRin37-S7D.

A)

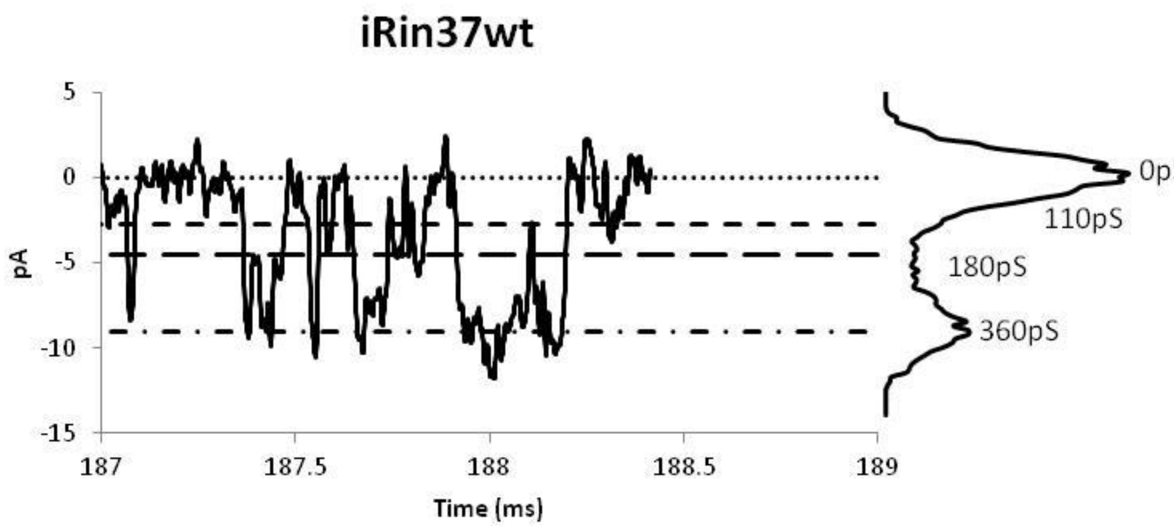

B)

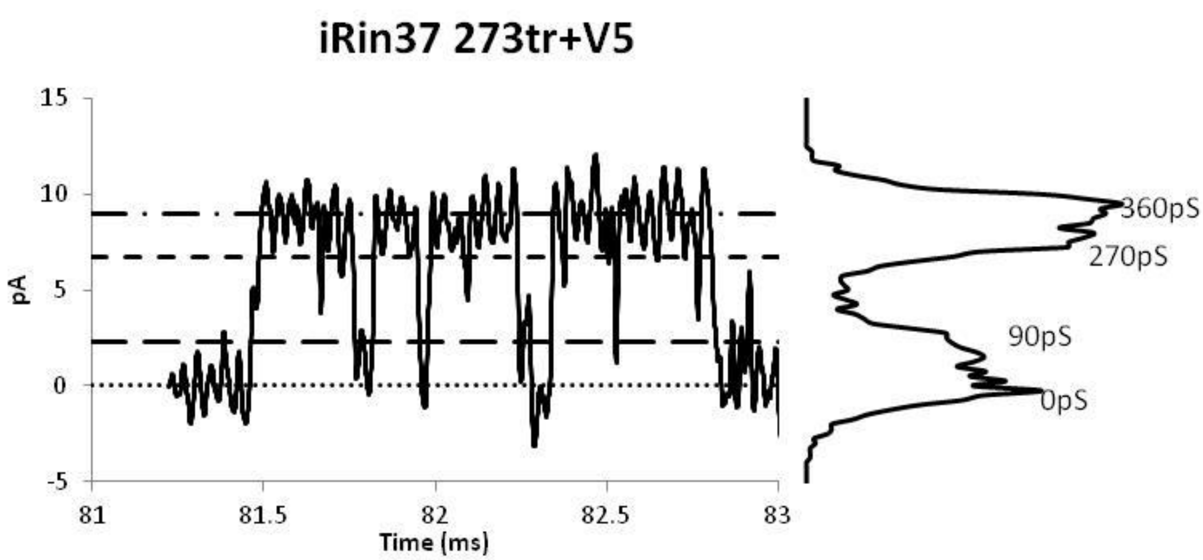

C)

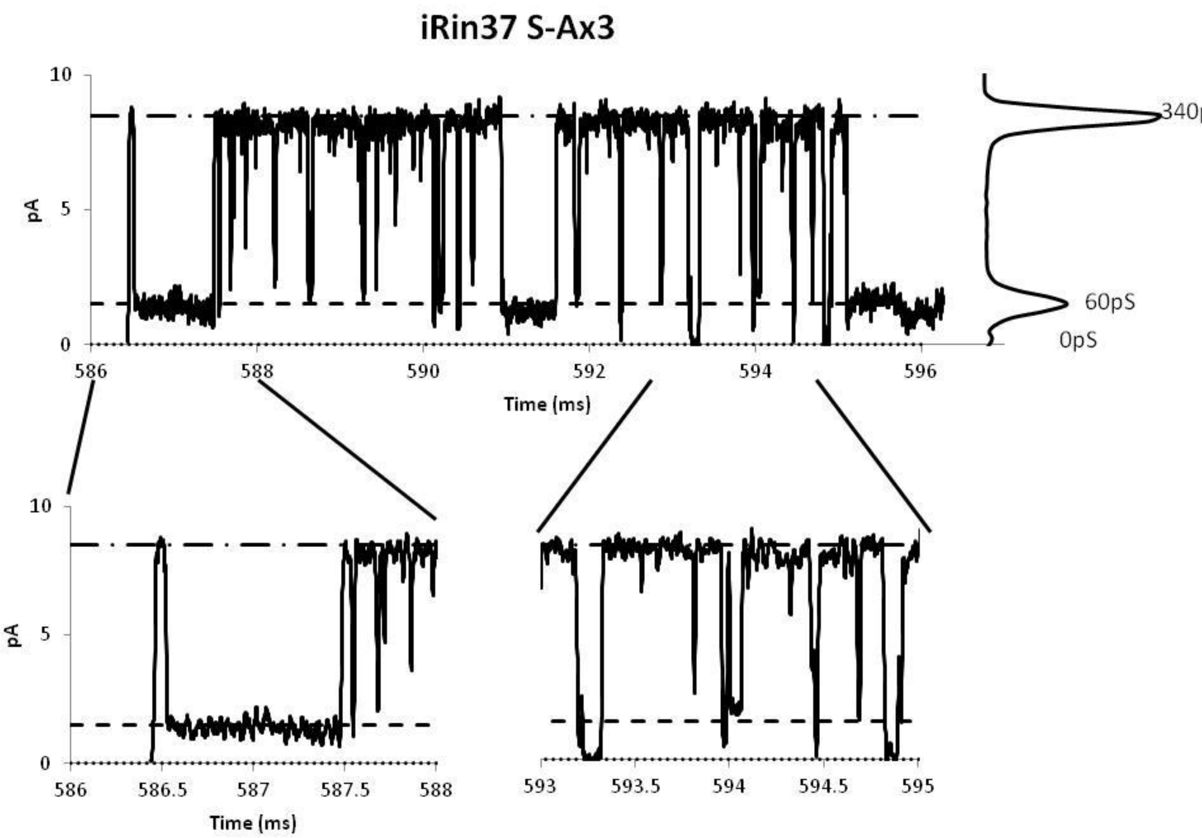
iRin37 S-Ax3
pA
Time (ms)
340pS
60pS
0pS
pA
Time (ms)

D)

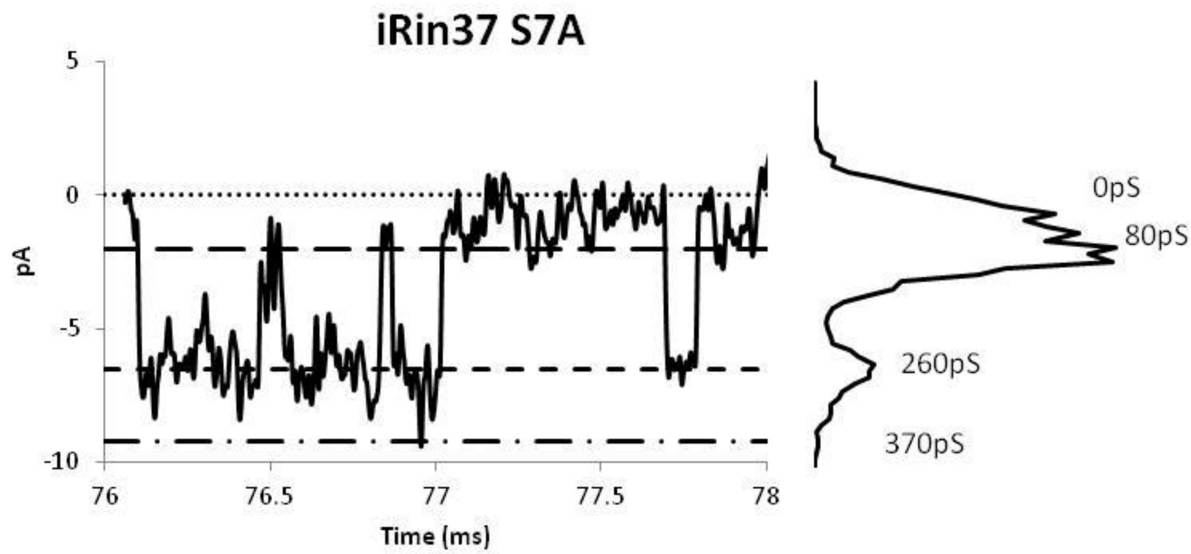
iRin37 S7A
pA
Time (ms)
0pS
80pS
260pS
370pS

E)

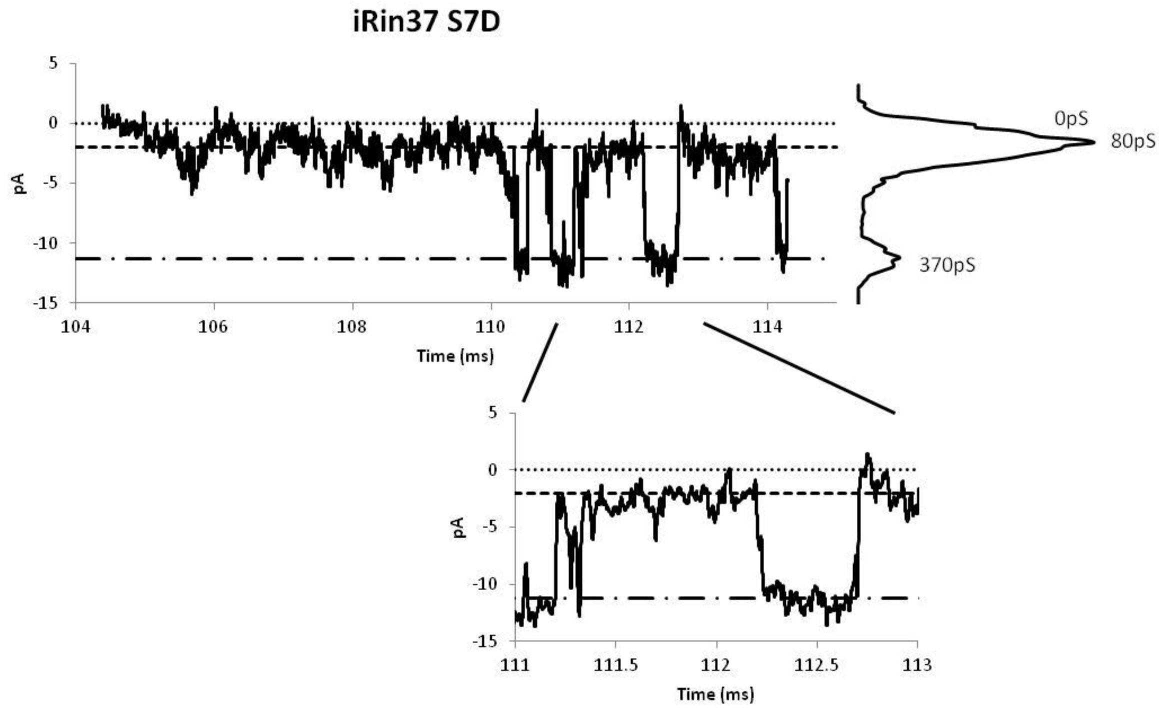

Figure 5. The phospho-mimetic S7D channel predominately resides in the low conductance state, similar to wt while the truncation and serine to alanine mutants shift towards a more fully open state. Relative frequencies are grouped in 10pS bins before being corrected for baseline A) 273tr B) S7A C) S7D D) S-Ax3

A)

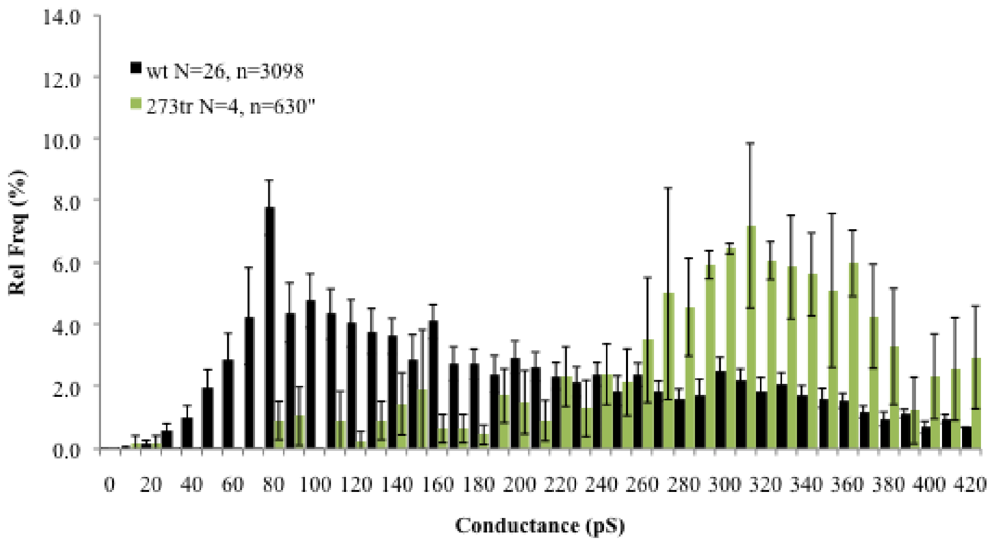

B)

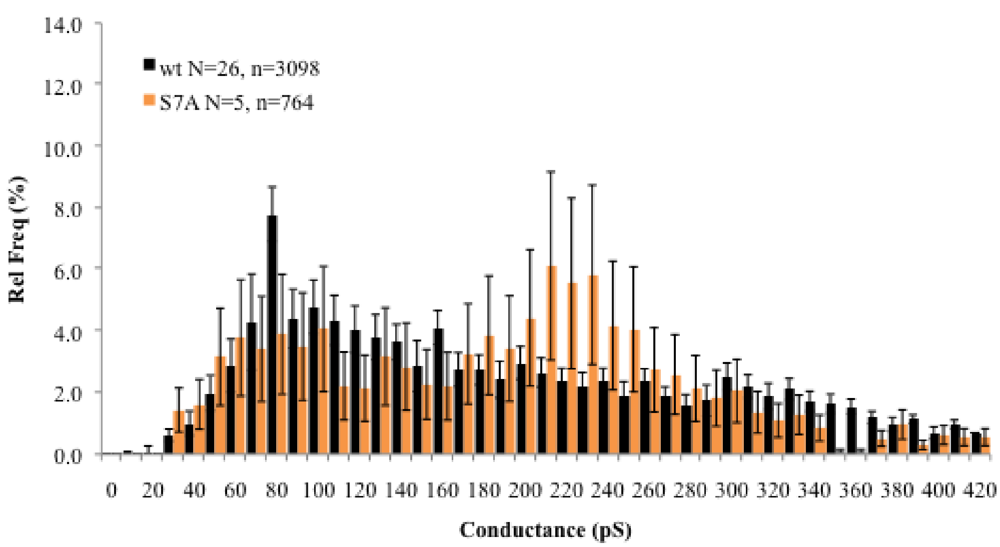

C)

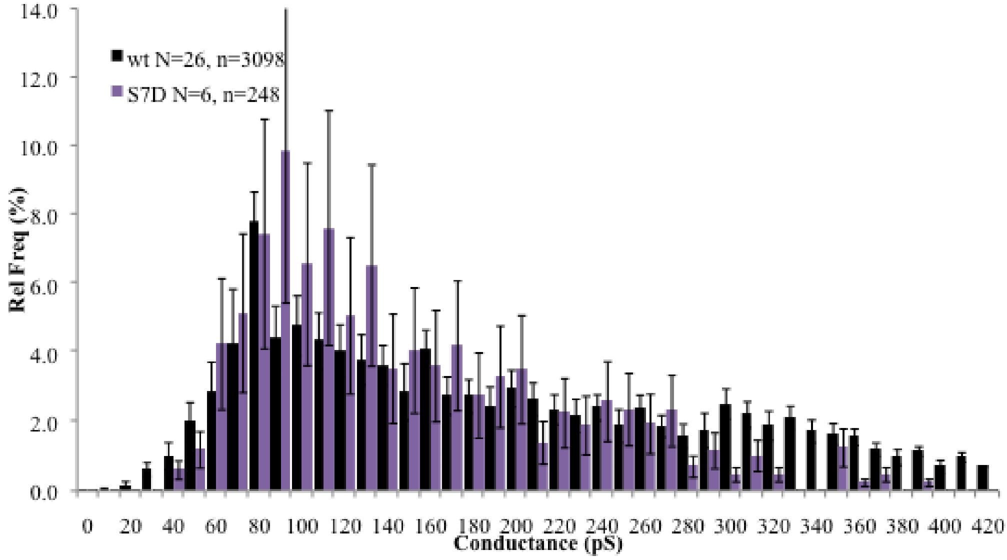

14.0
12.0
10.0
8.0
6.0
4.0
2.0
0.0
Rel Freq (%)
wt N=26, n=3098
S7D N=6, n=248
0 20 40 60 80 100 120 140 160 180 200 220 240 260 280 300 320 340 360 380 400 420
Conductance (pS)

D)

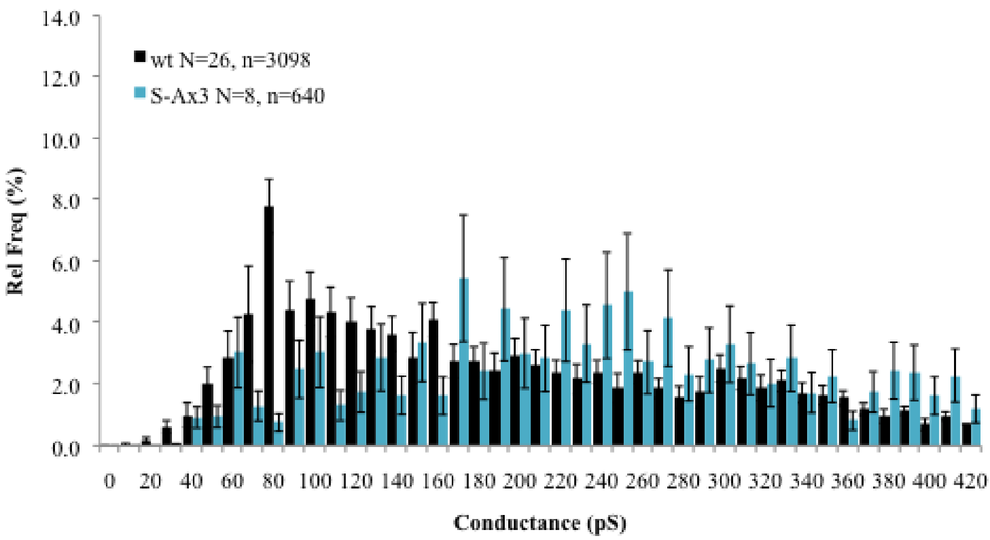

14.0
12.0
10.0
8.0
6.0
4.0
2.0
0.0
Rel Freq (%)
wt N=26, n=3098
S-Ax3 N=8, n=640
0 20 40 60 80 100 120 140 160 180 200 220 240 260 280 300 320 340 360 380 400 420
Conductance (pS)

Figure 6. Treatment of iRin37-wt with PKC agonist TPA resulted in an increased frequency of high conductance channels with a more open conformation and PKC inhibitor BIM prompted a high incidence of low conductance state channels adopting a more closed configuration. Relative frequencies have been corrected for baseline and grouped into 10pS bins. A) Cx37-wt + TPA B) Cx37-wt + BIM

A)

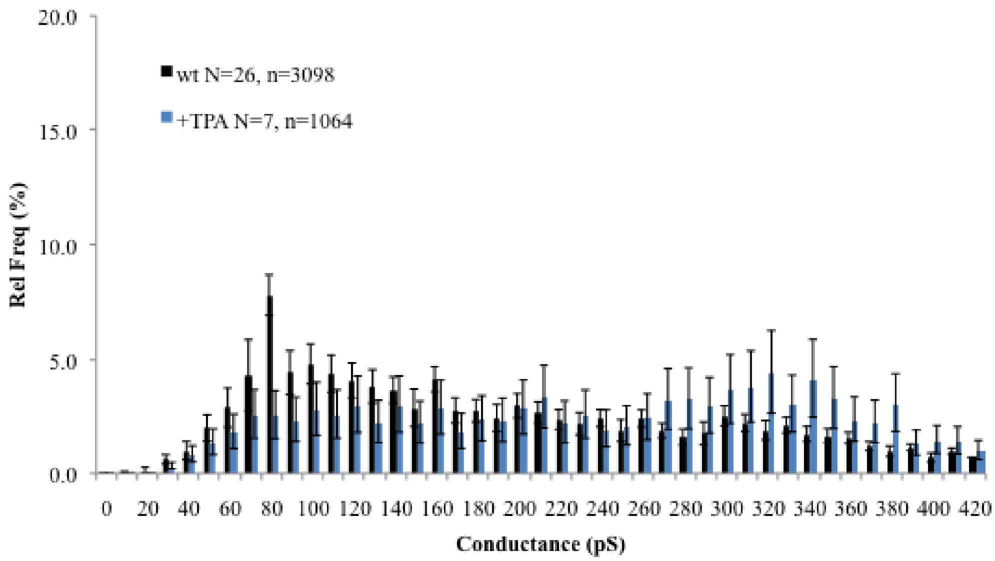

B)

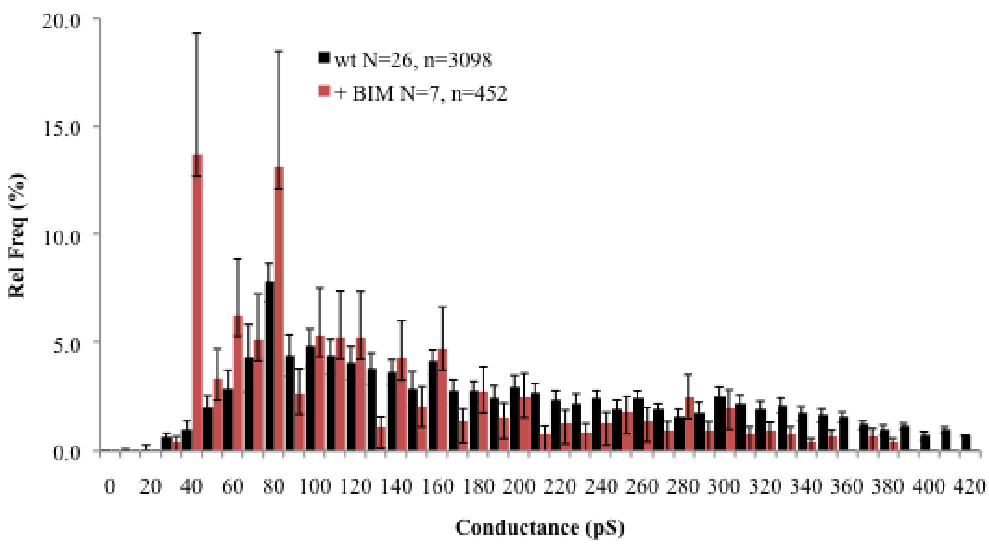

Figure 7. Proliferation is suppressed in both S7A and S7D cells while 273tr cells are growth permissive over a 21-day time period. While still growth inhibited, S-Ax3 escape the growth suppressive effect of Cx37 in Rin cells A) 273tr (n=3) B) S-Ax3 (n=3) C) S7A (n=4) D) S7D (n=4)

A)

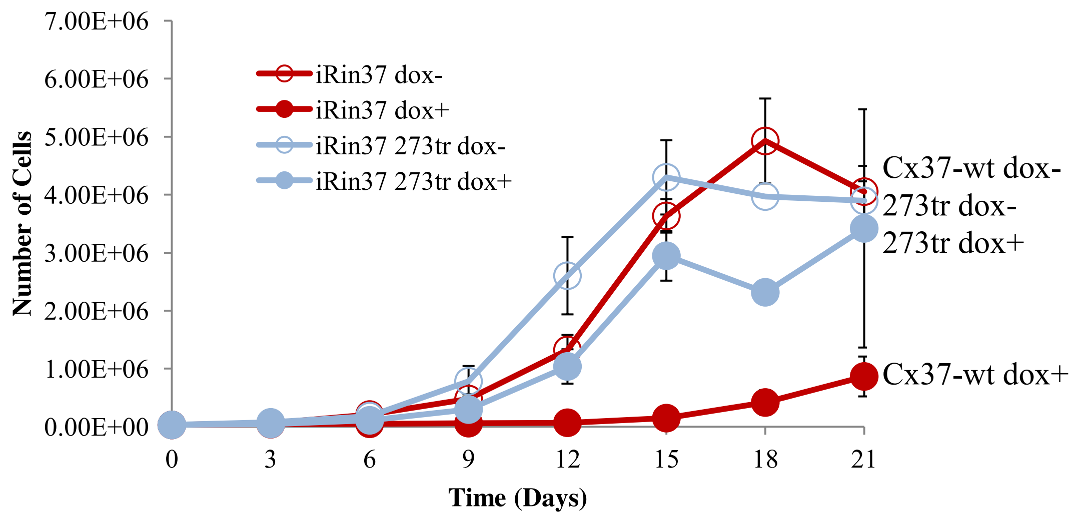

B)

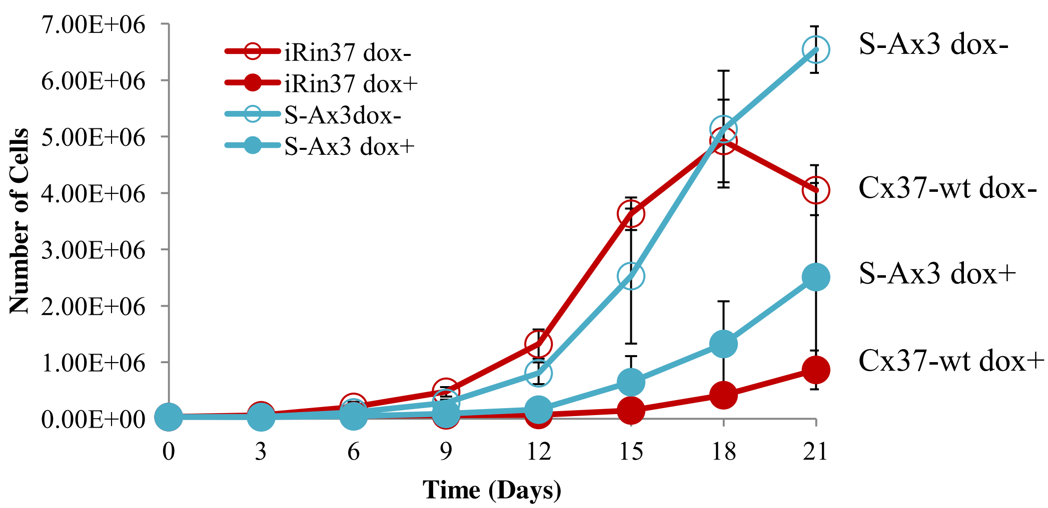

C)

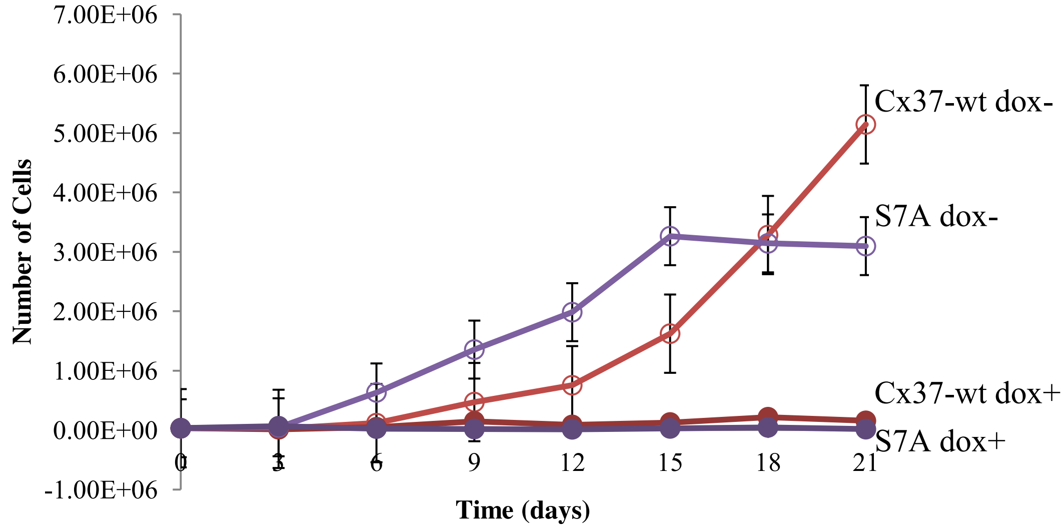
7.00E+06
6.00E+06
5.00E+06
4.00E+06
3.00E+06
2.00E+06
1.00E+06
0.00E+00
-1.00E+06
Number of Cells
0
3
6
9
12
15
18
21
Time (days)
Cx37-wt dox-
S7A dox-
Cx37-wt dox+
S7A dox+

D)

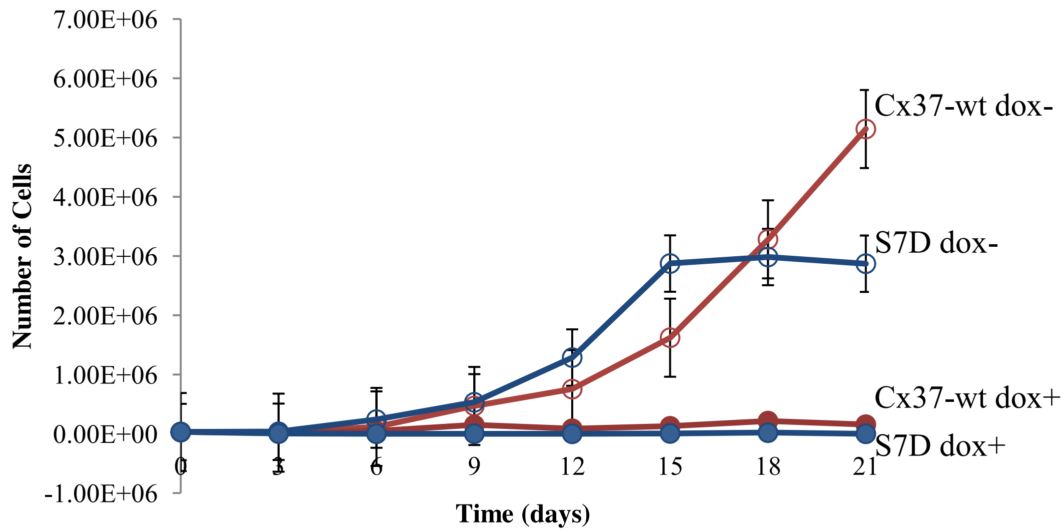
7.00E+06
6.00E+06
5.00E+06
4.00E+06
3.00E+06
2.00E+06
1.00E+06
0.00E+00
-1.00E+06
Number of Cells
0
3
6
9
12
15
18
21
Time (days)
Cx37-wt dox-
S7D dox-
Cx37-wt dox+
S7D dox+

Figure 9. After delayed induction of S7D expression (at day 12), S7D cells slow proliferation and possibly undergo cell death consistent with debris accumulation as revealed via FACS analysis (n=3). S7D dox -/+ cells were allowed to proliferate uninduced for 12 days before the addition of doxycyline to turn on Cx37-S7D expression.

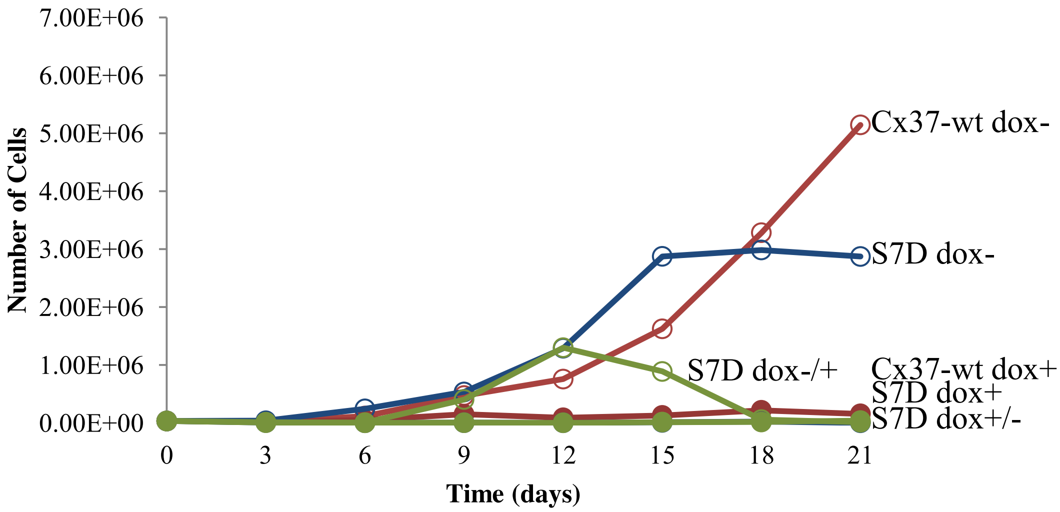

Figure 8. FACS analysis of cell cycle progression post serum deprivation of 72 hours of S7A and S7D mutants reveal growth arrest and possible apoptosis, respectively when protein expression is induced in the final 24 hours of serum deprivation (n=3). A) Cell cycle progression is stunted in S7A as seen by maintenance of phase distribution. 48 hours after serum return, S7D cell begins to accumulate debris indicated by an increase in S phase percentages. B) Cell cycle position of S7A and S7D cells at 24 and 48 hours show the accrual of debris in S7D cells beginning at 24 hours post serum return, which is absent in S7A cells.

A)

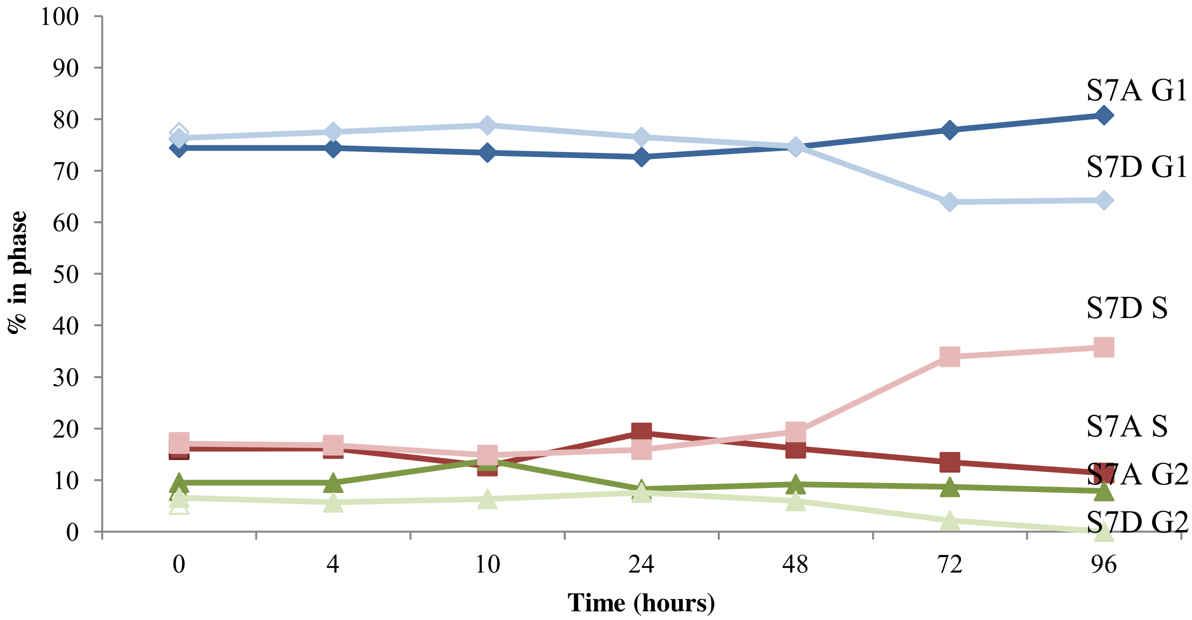

B)

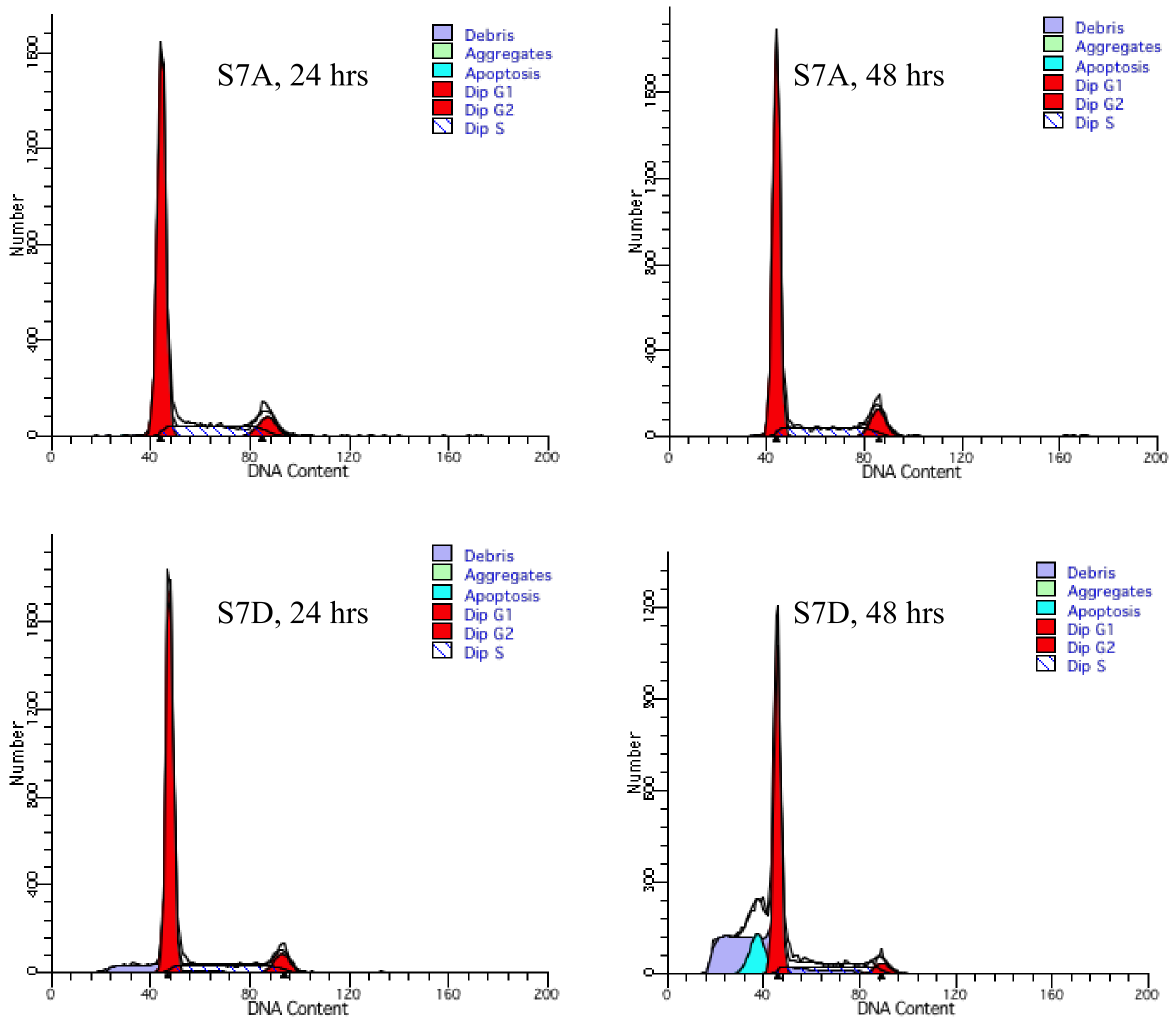
S7A, 24 hrs
S7A, 48 hrs
S7D, 24 hrs
S7D, 48 hrs
Debris
Aggregates
Apoptosis
Dip G1
Dip G2
Dip S
Number
DNA Content
0
40
80
120
160
200
400
800
1200
1600
300
600
900